Technical University of Denmark

DTU

Using a 1-D model to reproduce diurnal SST signals

Karagali, Ioanna; Høyer, Jacob L.

Published in:
Proceedings of the GHRSST XV Science Team Meeting

Publication date:
2014

Link back to DTU Orbit

DTU Library
Technical Information Center of Denmark

USING A 1-D MODEL TO REPRODUCE DIURNAL SST SIGNALS

Ioanna Kargali[(1)], Jacob L. Høyer[(2)]

(1) DTU Wind Energy, Technical University of Denmark, Risø Campus, Email: ioka@dtu.dk
(2) Centre for Ocean and Ice (COI), Danish Meteorological Institute (DMI), Email: jlh@dmi.dk

ABSTRACT

The diurnal variability of SST has been extensively studied as it poses challenges for validating and calibrating satellite sensors, merging SST time series, oceanic and atmospheric modelling. As heat is significantly trapped close to the surface, the diurnal signal's maximum amplitude is best captured by radiometers. The availability of infra-red retrievals from a geostationary orbit allows the hourly monitoring of the diurnal SST evolution. When infra-red SSTs are validated with in situ measurements a general mismatch is found, associated with the different reference depth of each type of measurement. A generally preferred approach to bridge the gap between in situ and remotely obtained measurements is through modelling of the upper ocean temperature. This ESA supported study focuses on the implementation of the 1 dimensional General Ocean Turbulence Model (GOTM), in order to resolve the diurnal signals identified from SEVIRI SSTs and in situ measurements. GOTM is a model solving the basic hydrodynamic and thermodynamic processes related to vertical mixing in the water column. From previous analysis it was shown that the data used to initialise the model, especially the temperature profiles, along with the selection of the coefficients for the 2-band parametrisation of light's penetration in the water column, hold a key role in the agreement of the modelled output with observations. To improve the surface heat budget and the distribution of heat, the code was modified to include an additional parametrisation for the total outgoing long-wave radiation and a 9-band parametrisation for the light extinction. New parametrisations for the stability functions, associated with vertical mixing, have been included. GOTM is tested using experimental data from the Woods Hole Oceanographic Institution Upper Ocean Processes Group archive. The successful implementation of the new parametrisations is verified while the model reproduces the diurnal signals seen from in situ measurements. Special focus is given to testing and validation of different set-ups using campaign data from the Atlantic Ocean, to establish a model set-up applicable to different regions.

1. Introduction

The diurnal cycle of SST occurs during day-time and under cloud-free conditions and is driven the concurrent occurrence of low enough wind (~<6 m/s) and strong solar heating. Due to lack of wind that promotes mixing, heat is trapped in the upper ocean layer creating a stratified, warm layer which extends from the surface to a few meters depth with temperature increased by potentially several degrees. Diurnal warming has been extensively identified with the use of SST retrievals obtained from radiometers on space-borne platforms, which correspond to skin and sub-skin temperatures, i.e. in the upper mm of the water column. It has been identified in various locations in the global ocean (Stuart-Menteth et al., 2003) and more recently, at the higher latitudes of the North Hemisphere (Karagali et al., 2012) and the entire Atlantic Ocean including the enclosed basins (Karagali and Høyer, 2014).

Diurnal variability of SST can cause complications in various research areas. For example, in an attempt to create long and stable temperature records for climate studies, merging SST time-series from different satellite sensors typically occurs but these have different overpass times therefore capture different parts of the diurnal cycle which needs to be known. When developing retrieval algorithms for radiometers, diurnal variability should be removed from buoy observations that are used for validation purposes. Diurnal changes in SST will drive variations in the instantaneous values of the air-sea heat fluxes (Clayson and Bogdanoff, 2013) and the atmospheric stability, and since this effect is typically not taken into account in ocean and atmospheric models, forecast skill may be reduced. In an attempt to understand and predict diurnal variability, modelling efforts have been undertaken by the community, developing various physical mixed layer models and parametrisations; an extensive review of such activities is available from Kawai and Wada (2007). Karagali and Høyer (2013) tested some parametrisations in the North and Baltic Seas and compared them with SEVIRI derived diurnal warming estimates, highlighting the dependence of the parametrisations on their input fields, typically from NWP models which do not resolve the diurnal SST cycle.

This study utilises the General Ocean Turbulence Model (GOTM) for the purpose of reproducing the diurnal signals seen from in situ instruments and satellite SSTs. Sensitivity tests were performed in order to investigate the impact of the various GOTM parameters in the model's skill to reproduce the daily SST

cycles. Section 2 gives a description of the model, the experimental set-up and the data sets used for the model tests. The results are presented in section 3 and main conclusions are drown in section 4.

2.   Experimental Set-Up

GOTM is a 1 dimensional turbulence model that describes the basic thermodynamic and hydrodynamic processes related to the vertical mixing by solving the 1-d equations for the transportation of heat, salt and momentum (Umlauf et al.). Surface fluxes can be either prescribed from NWP models or calculated by GOTM with the use of bulk flux algorithms which require the input of meteorological variables such as the 10-m wind components, the air temperature, pressure, humidity and cloud cover. The model includes a 2-band parametrisation for the light extinction inside the water column but has been modified to also include a 9-band parametrisation. Additional options have been included for i) the calculation of the net long-wave radiation by means of a Brunt type formula and ii) the prescription of the down-welling long wave radiation from measurements. New stability functions, i.e. dimensionless quantities involved in the expressions for the diffusivity of heat and momentum, have also been added. The vertical grid extends down to a depth of 150 m, using 150 vertical layers of which approximately 70 are in the upper 10 m. For this study, the model is assessed at 3 different locations, shown in Figure 1. Depending on the location at which the model is assessed, different set-up options were investigated as shown in Table 1.

Parameter	Options
1. Down-welling Long-wave Rad.	1. Clark et al., 1974
	2. Hastenrath & Lamb, 1978
	3. Bignami et al., 1995
	4. Berliand & Berliand, 1952
	6. User prescribed
2. Light Extinction Scheme	1. 2-band (J I)
	2. 2-band (J I, upper 50 m)
	3. 2-band (J IA)
	4. 2-band (J IB)
	5. 2-band (J II)
	6. 9-band (Paulson & Simpson, 1981)
	7. 9-band (Paulson & Simpson, 1981 and COART)
	8. 9-band (Paulson & Simpson, 1981 and MODTRAN)

Table 1: GOTM set-up options evaluated in this study.

2.1 Arctic Diurnal Warming

In Eastwood et al. (2011), a diurnal warming event in the order of 3 degrees was identified in the Arctic, around 74.4 N and 44.5 E, during the 21st to 22nd of June 2008. According to evidence from satellite SSTs, the foundation temperature was 3 °C and reached up to 6 °C at mid-day. This event was modelled using fluxes calculated with the Fairall algorithm (embeded in GOTM), from meteo-files obtained from the HIRLAM NWP model which were provided by the Norwegian Meteorological Institute (metNo). Climatological temperature profiles from the World Ocean Atlas 09 (WOA09) were used to initialise the model, along with

temperature profiles from an ocean model available at metNo. The WOA09 dataset was obtained through the National Oceanic Atmospheric Administration (NOAA) National Oceanographic Data Center (NODC) and can be found at http://www.nodc.noaa.gov/OC5/WOA09/pr_woa09.html.

2.2 Marine Light – Mixed Layer 1991 Experiment (MLML91)

The MLML91 experiment took place during the spring and summer of 1991, when a buoy was moored at 59.5 N and 20.82 W at 2822 m of water, measuring meteorological variables such as temperature, humidity, pressure, wind, down-welling long-wave and short-wave radiation and water temperature down to a depth of 325 m. The data were obtained from the Woods Hole Oceanographic Institute Upper Ocean Processes working group and are publicly available at http://uop.whoi.edu/archives/mlml91/mlml91.html. A period of 4 days, from the 29th of June to the 2nd of July 1991, during which a 1 degree event occurred was modelled using the buoy meteo and ocean measurements as input fields. During the modelling experiment, two methods for the down-welling long-wave radiation were tested and 8 methods for the calculation of the light extinction within the water column (see Table 1).

2.3 PIRATA Moored Buoy

The PIRATA mooring is located at 15°N, 38°W. The buoy is equipped with instrumentation for measuring various meteorological parameters such as air temperature, humidity, pressure, wind, down-welling long-wave and short-wave radiation and water temperature at different depths. Approximately 1 year of measurements were obtained from the Pacific Marine Environmental Laboratory (PMEL) through the Tropical Atmosphere Ocean (TAO) project and are available at http://www.pmel.noaa.gov/tao/disdel/disdel-pir.html. The event occuring on the 24/8/2006, reached 1.5 degrees amplitude, and in this study the period from the 22nd to the 25th of August was modelled using the different options shown in Table 1.
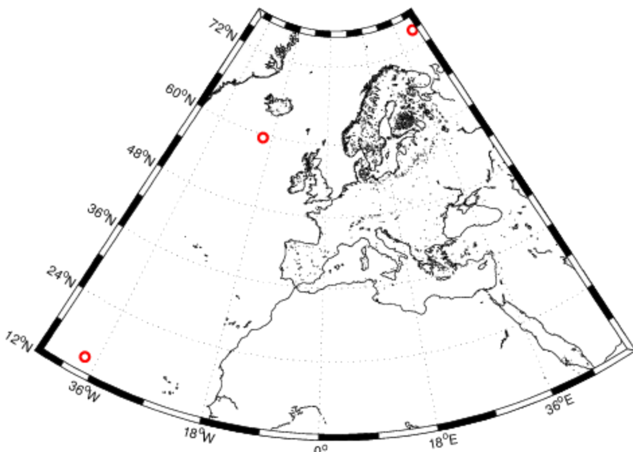

Figure 1: Locations used for the GOTM runs. Starting from the top right, the diurnal warming event identified in Eastwood et al. 2008, in the middle is the MLML91 moored buoy and bottom left the moored PIRATA buoy.

3.   Results

The diurnal warming event in the Arctic, identified in Eastwood et al. (2011) had an amplitude of 3 degrees, at the warmest spot, and occurred on the 22nd of June 2008. For this study, the temperature at the location 74.4 N, 44.5 E was modelled using NWP meteorological parameters, allowing for the calculation or prescription of the short-wave radiation, different parametrisations for the long-wave radiation, different temperature profiles and LE schemes. Figure 2 shows the test runs, where the 1st day is used as spin-off period. In the left panel, the coloured lines show the top layer GOTM temperature estimated using calculated (solid) versus prescribed (dashed) short-wave radiation and parametrisation 2 (red) versus 4 (cyan) for the long-wave radiation calculation. For these 4 curves, one initial temperature profile from the World Ocean Atlas 09 dataset was used. What is generally seen is that there is a mismatch in the timing of the diurnal cycle, associated with the difference reference time of the HIRLAM input field. A very small difference between the long-wave radiation parametrisations is identified. Moreover, it is found that the WOA09 profile has a lower top layer temperature than what was observed from the satellite SSTs (3 °C) and that the runs using this profile, had an amplitude of approximately 2 °C. The black solid line shows the GOTM temperature

modelled by calculating the short-wave radiation, using parametrisation 1 for the long-wave radiation and a temperature profile from the metNo ocean model. The red and cyan dashed-dotted lines use the same methods for the short-wave radiation and temperature profile but different parametrisations for the long-wave radiation. The main finding from this comparison is that with the appropriate initial temperature profile, the amplitude of the diurnal event is better resolved reaching up to 6 °C. Moreover, parametrisations 1 and 4 for the long-wave radiation produce the same result. The black dashed line has the same set-up as the black solid line, except that it uses a modified WOA09 profile in that the top level has been adjusted to the value of the metNo profile. By comparing the black solid and dashed curves, it is found that it is not only the top layer of the initial temperature profile that regulates the modelled temperature, but also the deeper layers. The right panel of Figure 2 shows the temperature evolution for GOTM runs using a calculated short-wave radiation, parametrisations 1.1 (red lines) and 1.3 (cyan lines) for the long-wave radiation, and LE schemes 2.1 (solid), 2.2 (dashed), 2.3 (dashed-dotted) and 2.4 (diamonds). It is shown that for a given colour, i.e. long-wave radiation parametrisation, the highest amplitude arises when using the LE 2.1 scheme, representative of open ocean waters. Moreover, for any given LE scheme option the long-wave parametrisation 1.1 yields higher temperatures compared to 1.3. In addition for a given colour, all LE schemes provide temperature curves that differ in amplitude during the warming and peak amplitude phase but collapse on each other during the night-time cooling period, except option 2.3 which yields lower temperatures consistently throughout the modelling period.
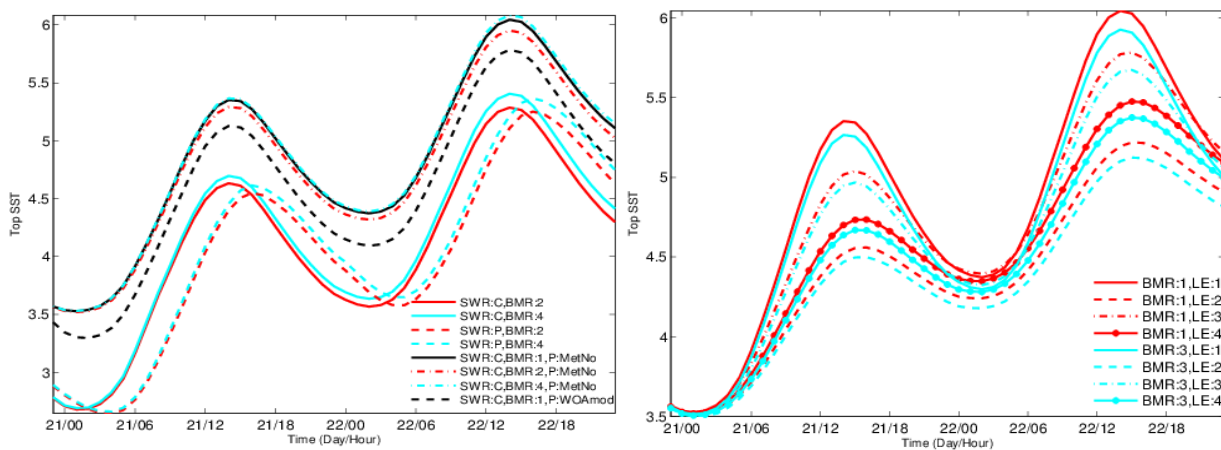

Figure 2: Temperature evolution for the 2 day period of the Arctic warming event, using different methods for the fluxes and different profiles (left), different light extinction schemes (right).

A warming event of 1 K was identified in the 2m temperature time-series of the MLML91 measurements and was used as a test case for the GOTM set-up. The evolution of temperature between the 29th of June and the 2nd of July 1991 from the buoy (black crosses) and the GOTM runs (coloured lines) using different LE schemes are shown in Figure 3. It is found that while GOTM reproduces rather well the diurnal variability of the first 2 days, it generally fails to reproduce the much smaller variability seen in the last 2 days of measurements. Prescribing the long-wave radiation (option 1.2, right panel) adds more variability in the daily cycle, particularly in the last day. The amplitude of the main event, on the 2nd day, is well captured particularly from the 9-band model (blue lines). The statistics between the GOTM and buoy temperature at 2m are shown in Table 2, for the various GOTM set-ups. Generally, lower mean biases (μ) and standard deviations (σ) and higher correlation coefficients (r) were estimated for the GOTM runs using the prescribed long-wave radiation (option 1.6). When examining the differences due to the light extinction schemes, the lowest μ is found for option 2.8 (the 9-band model with coefficients from Paulson and Simpson (1981) and attenuation lengths from the MODTRAN model) while the lowest σ and highest r values are found for 2.5 (the 2 band model with Jerlov II type water). Nonetheless, the difference in the σ between LE schemes is in the order of 0.03 degrees.

At the PIRATA site, the 1m buoy and GOTM temperatures for the 2 options of the long-wave radiation and the different LE schemes are shown in Figure 4. GOTM reproduces the diurnal variability seen in the measurements, independent of the long-wave radiation method or the LE scheme. Minor differences between the amplitudes reached using the various LE schemes are identified, but they are mostly in the order of 0.2-0.3 K. The 9-band model (blue lines) performs better at capturing the amplitude of the peak event but does slightly overestimate the warming during the first two days and the last.
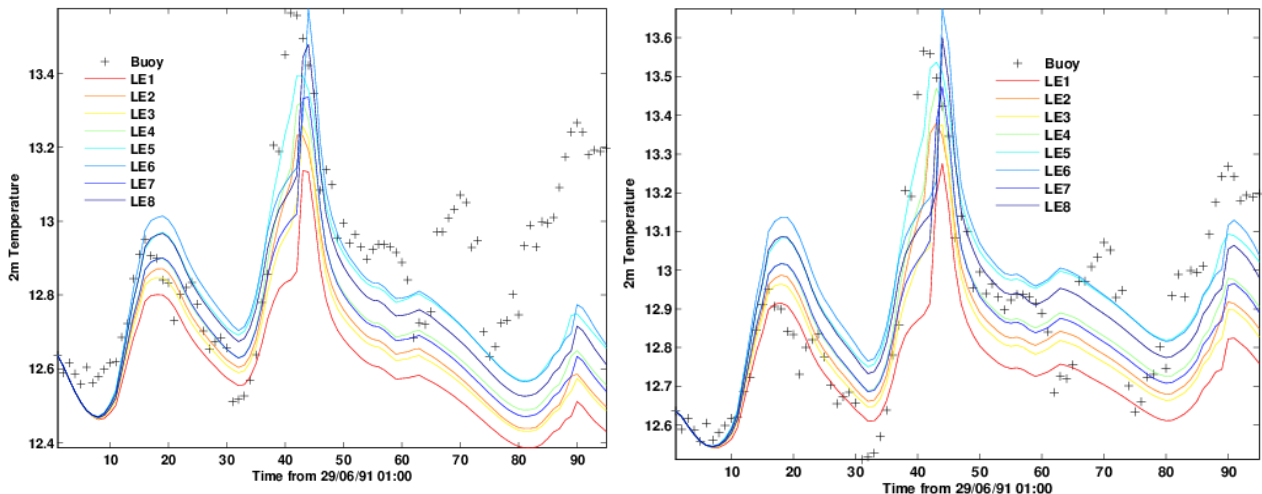
Figure 3: Temperature evolution for the 4 day period of the MLML91 warming event, using 2 different methods for the down-welling long-wave radiation, i.e. the Berliand and Berliand (1952) parametrisation (left) and the measurements from the buoy (right). The coloured lines represent different LE schemes and the crosses are the buoy measured temperature at 2m.

LE	Mean Bias (μ)		Stand. Dev. (σ)		Corr. Coef. r	
	1.4	1.6	1.4	1.6	1.4	1.6
2.1	-.29	-.15	.23	.18	.41	.71
2.2	-.23	-.07	.22	.15	.53	.81
2.3	-.25	-.10	.22	.16	.51	.78
2.4	-.19	-.04	.20	.14	.59	.83
2.5	-.11	.05	.19	.13	.66	.85
2.6	-.10	.05	.21	.16	.59	.76
2.7	-.20	-.05	.22	.16	.53	.76
2.8	-.14	.01	.21	.16	.59	.77

Table 2: Statistics of the GOTM-Buoy 2m temperature for the different runs. The rows represent different LE schemes from 1 to 8, while the internal columns are for the GOTM runs with options 4 and 6 for the down-welling long-wave radiation.

The statistics between the buoy and GOTM temperatures are shown in Table 3, indicating generally lower μ and σ and higher r values for option 1 of the long-wave radiation (the parametrisation of Berliand and Berliand, 1952). Nonetheless, the differences in the statistics between the 2 options are minor and in the order of 0.08 K. When examining the statistics due to the different LE schemes, option 3 (2-band model using the Jerlov IA type) shows the lowest μ and σ and highest r value when the long-wave radiation is parametrised using the Berliand & Berliand, 1952 formula (option 1.4) and option 1 (2-band model using Jerlov I type) when the long-wave radiation is prescribed (1.6). When the top layer temperature from GOTM (1.5 cm) is compared to the SEVIRI extracted temperature, shown in Figure 5, it is found that SEVIRI shows much colder temperatures during night-time (almost 2 degrees difference) and higher day-time temperatures (by approximately 1 degree) during the 1st day. The night-time cooling at the beginning of the 2nd day is approximately 1 degree larger in the SEVIRI SST, but the 2nd day peak is reasonably resolved. Unfortunately, the 3rd day large diurnal warming event is absolutely missed by SEVIRI. This highlights the difficulty of collecting appropriate datasets with full observations from in-situ and satellite sensors for the purposes of calibrating the GOTM model.
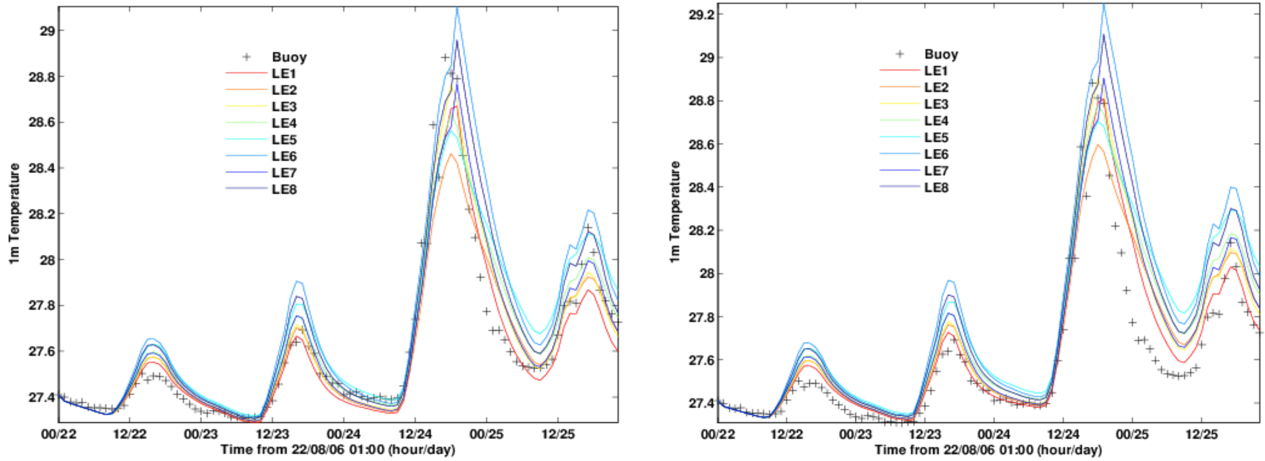
Figure 4: Temperature evolution for the 4 day period of the PIRATA warming event, using 2 different methods for the down-welling long-wave radiation, i.e. the Berliand and Berliand (1952) parametrisation (left) and the measurements from the buoy (right). The coloured lines represent different LE schemes and the crosses are the buoy measured temperature at 1m.

LE	Mean Bias (μ)		Stand. Dev. (σ)		Corr. Coef. r	
	1.4	1.6	1.4	1.6	1.4	1.6
2.1	-.03	.05	.08	.09	.97	.97
2.2	-.01	.06	.11	.11	.96	.94
2.3	.01	.09	.08	.12	.97	.96
2.4	.03	.11	.10	.13	.96	.95
2.5	.07	.15	.13	.16	.93	.92
2.6	.11	.19	.15	.19	.95	.94
2.7	.02	.09	.10	.13	.96	.95
2.8	.07	.15	.12	.16	.95	.96

Table 3: Statistics of the GOTM-Buoy 1m temperature for the different runs during the period 22-25/8/2006 at the PIRATA buoy location. The rows represent different LE schemes from 1 to 8, while the internal columns are for the GOTM runs with options 1 and 2 for the down-welling long-wave radiation.
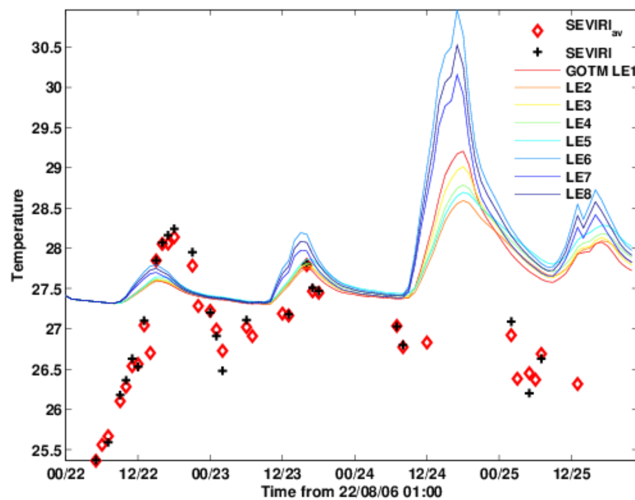

Figure 5: Top layer GOTM modelled temperatures using the prescribed long-wave radiation and different LE schemes (coloured lines) and SEVIRI retrieved SST from the grid cell (black crosses) containing the PIRATA buoy and from the average of 4 grid cells around the PIRATA location (red diamonds).

4.   Conclusion

This study has focused on applying a 1 dimensional ocean turbulence model for the purpose of reproducing diurnal signals in the sea surface temperature as seen from in situ measurements and satellite SST fields. A variety of tunable model parameters were tested and their impact in GOTM's skill to reproduce sea water temperatures comparable to the observations was evaluated in terms of the mean bias, standard deviation and correlation coefficient.

Three different locations representative of different latitudinal bands were tested, including the Arctic Ocean, the mid/high latitudes and Tropics of the Atlantic Ocean. Regarding the parametrisation for the short-wave radiation, it was found from sensitivity tests that certain options yield almost the results (1 and 4) while others (2 and3) show a small reduction in the amplitude of the diurnal signal in the order of 0.1-0.2 degrees, at least in the Arctic case. Prescribing the long-wave radiation from measurements does not always yield the best results, likely due to errors in the measurements themselves, but such data are not always available.

Regarding the different light extinction schemes, it was found that the 9-band model, which is thought to be more representative of the physical conditions that occur when light enters the water column, did not always yield better results compared to the 2 band model. Nonetheless, the error statistics for the 9-band modle were only approximately 0.05 degrees higher compared to the selection with the lowest bias and standard deviation and the highest correlation coefficient.

It has been shown that GOTM reproduces very well the diurnal signals seen from measurements and that further refinements can improve the model's performance. So far, the model has been driven with in situ measurements and the results are promising, but when the model is initialised with NWP fields, its performance against in situ data may degrade.

5.   References

Berliand, M. E. and T. G. Berliand, Determining the net long-wave radiation of the Earth with consideration of the effect of cloudiness, Isv. *Akad. Nauk. SSR Ser. geofiz* **No. 1**, 1952.

Clayson, C. A. and A. S. Bogdanoff, The effect of diurnal sea surface temperature warming on climatological air-sea fluxes, *J. Climate* **26**, 2546-2556, 2013.

Eastwood, S., Le Borgne, P., Péré, S. and D. Poulter, Diurnal variability in sea surface temperature in the Arctic, *Remote Sens. Environ.* **115**, 2594-2602, 2011.

Kawai, Y. and A. Wada, Diurnal sea surface temperature variation and its impact on the atmosphere and ocean: a review, *J. Oceanogr.* **63**(5), 721-744, 2007.

Karagali, I., Høyer J. L. and C. B. Hasager, SST diurnal variability in the North Sea and the Baltic Sea, *Remote Sens. Environ.* **121**, 159-170, 2012.

Karagali, I. And J. L. Høyer, Observations and modelling of the diurnal SST cycle in the North and Baltic Seas, *j. Geophys. Res.* **118**, 4488-4503, 2013.

Karagali, I. and J. L. Høyer, Characterisation and quantification of regional diurnal SST cycles from SEVIRI, *Ocean Sci. Discuss.* **11**, 1093-1128, 2014.

Paulson, C. A. and J. J. Simpson, The Temperature Difference Across the Cool Skin of the Ocean, *J. Geophys. Res.* **86** (C11)**,** 11044-11054**,** 1986.

Stuart-Menteth, A. C., Robinson, I. S., and P. G. Challenor, A global study of diurnal warming using satellite-derived sea surface temperature. *J Geophys. Res.* **108** (C5), 3155, 2003.

Umlauf, L., Burchard, H. and K. Bolding, GOTM Source Code and Test Case Documentation, Developer's version 4.1, available http://www.gotm.net/index.php?go=documentation.